

## THE AXISYMMETRIC STELLAR WIND OF AG CARINAE<sup>1</sup>

REGINA E. SCHULTE-LADBECK

Department of Physics and Astronomy, University of Pittsburgh, 3941 O'Hara Street, Pittsburgh, PA 15260  
 rsl@binar.phyast.pitt.edu

GEOFFREY C. CLAYTON

Center for Astrophysics and Space Astronomy, University of Colorado, Campus Box 389, Boulder, CO 80309  
 gclayton@fenway.colorado.edu

D. JOHN HILLIER

Department of Physics and Astronomy, University of Pittsburgh, 3941 O'Hara Street, Pittsburgh, PA 15260  
 djh@minerva.phyast.pitt.edu

AND

TIM J. HARRIES AND IAN D. HOWARTH

Department of Physics and Astronomy, University College London, Gower Street, London WC1E 6BT, U.K.  
 th@starlink.ucl.ac.uk, idh@starlink.ucl.ac.uk

Received 1993 November 16; accepted 1994 January 14

### ABSTRACT

We present optical linear spectropolarimetry of the Luminous Blue Variable AG Carinae obtained after a recent visual brightness increase. The absence of He II  $\lambda 4686$  emission, together with the weakening of the He I spectrum and the appearance of Fe lines in the region around 5300 Å, confirm that AG Car has started a new excursion across the HR diagram.

The H $\alpha$  line profile exhibits very extended line wings that are polarized differently in both amount and position angle from either the continuum or the line core. The polarization changes across H $\alpha$ , together with variable continuum polarization, indicate the presence of *intrinsic* polarization. Coexistence of the line-wing polarization with extended flux-line wings evidences that both are formed by electron scattering in a dense wind. The position angle rotates across the line profiles, in a way that presently available models suggest is due to rotation and expansion of the scattering material.

AG Car displays *very large* variations of its linear polarization with time,  $\Delta P \sim 1.2\%$ , indicating significant variations in envelope opacity. We find that the polarization varies along a preferred position angle of  $\sim 145^\circ$  (with a scatter of  $\pm 10^\circ$ ) which we interpret as a symmetry axis of the stellar wind (with an ambiguity of  $90^\circ$ ). This position angle is co-aligned with the major axis of the AG Car ring nebula and perpendicular to the AG Car jet. Our observations thus suggest that the axisymmetric geometry seen in the resolved circumstellar environment at various distances already exists within a few stellar radii of AG Car.

From the H $\alpha$  polarization profile we deduce an interstellar polarization of  $Q = 0.31\%$ ,  $U = -1.15\%$  at H $\alpha$ . The inferred interstellar polarization implies that the intrinsic polarization is not always of the same sign. This indicates either significant temporal changes in the envelope geometry, or it may arise from effects of multiple scattering in conjunction with density variations.

*Subject headings:* polarization — stars: evolution — stars: individual (AG Carinae) — stars: mass-loss — supergiants

### 1. INTRODUCTION

Luminous Blue Variables (LBVs; Conti 1984) are early-type supergiants that undergo photometric and spectroscopic variations on a variety of magnitude scales and timescales. LBVs cycle across the upper part of the Hertzsprung-Russel (H-R) diagram varying both in visual magnitude and spectral type. As an LBV grows brighter its equivalent spectral type becomes later. During the brightening phase the most luminous LBVs cross the observed upper luminosity boundary of the H-R diagram known as the Humphreys-Davidson limit (Humphreys & Davidson 1979) into a temperature-luminosity region otherwise void of stars.

The variability of the Galactic LBV AG Car was recently summarized by Nota et al. (1992). Apart from a single gigantic outburst  $\sim 10^4$  yr ago, inferred from the presence of a ring nebula, AG Car displays LBV cycle-type variability on a time-scale of  $\sim 10$  yr, and erratic micro-variability on shorter time-scales. The LBV-cycle variations of AG Car range from typically 9 to 6.5 mag in visual magnitude and are associated with changes in spectral type from O/WN (a “slash” star) or B1 I to A0 I (Stahl 1987; Caputo & Viotti 1970). The changes in the UV-to-IR flux distribution between minimum and maximum state have been interpreted to take place at a constant bolometric luminosity (Viotti et al. 1984), implying that the radius of the photosphere changes, by a factor of  $\sim 10$ . LBV variations are generally believed to be caused by an unknown type of instability involving large variations (factor of 10) in the mass-loss rate (see Lamers & de Loore 1987;

<sup>1</sup> Based on observations collected at the Anglo-Australian Telescope which is operated by the Anglo-Australian Observatory.

Leitherer et al. 1989), but in AG Car the mass-loss rate appears to be stable, of order  $10^{-4} M_{\odot} \text{ yr}^{-1}$ , even during the transition from minimum to maximum (Hillier 1992; Leitherer, Neto, & Schmutz 1992b). AG Car has been in minimum since 1985. Our observations straddle the onset of a brightening to a possible new maximum (Kilmartin & Bateson 1991).

AG Car is physically associated with an elliptical ring nebula best seen in images taken through emission-line filters (Thackeray 1950, 1977; Smith 1991; Stahl 1987; Nota et al. 1992). The appearance of the nebula is reminiscent of that of classical planetary nebulae. The ring structure as a whole is box-shaped, displays an inhomogeneous surface-brightness distribution, and has a width of a few arcseconds. The major axis of the ring has an outer radius of  $\sim 20''$  and is located at a position angle (P.A.) of  $\sim 135^{\circ}$ . Portions near the minor axis, which has an extension of  $\sim 15''$ , appear to be brighter. The bright regions are located at P.A.s  $\sim 35^{\circ}$  and  $\sim 225^{\circ}$  coincident with the directions of the bipolar jet (see below). Far-IR radiation peaks at a distance of  $\sim 9''$  in the same direction (McGregor et al. 1988) and is due to thermal dust radiation. Dust-reflected starlight from the nebula is apparent in *IUE* UV spectra (Viotti et al. 1988). Optical long-slit spectroscopy revealed that the nebula is a hollow, ellipsoidal shell expanding at a velocity of  $\sim 70 \text{ km s}^{-1}$  (Smith 1991; Nota et al. 1992), and that it was ejected in a single outburst. The luminosity of AG Car (based on a distance of  $\sim 6 \text{ kpc}$ ; Humphreys et al. 1989) suggests that AG Car has never passed through a red supergiant phase, but has evolved with considerable mass loss in the blue part of the Hertzsprung-Russell diagram (Nota et al.; but see Robberto et al. 1993). Support for extensive mass loss is provided by de Freitas Pacheco et al. (1992), who find that the nebula shows evidence for CNO-processed material (but see Mitra & Dufour 1990). In addition to the ring nebula, the star is surrounded by extended, faint nebulosity detected in  $\text{H}\alpha$  out to  $45''$  (de Freitas Pacheco et al.).

Using coronagraphic imaging, Paresce & Nota (1989) discovered intricate bipolar structures near the stellar image inside of the ring nebula, which are commonly referred to as the AG Car jet. The north-eastern jet is a detached feature located between P.A.s of  $23^{\circ}$  to  $35^{\circ}$  at distances of  $\sim 10''$  to  $13''$  from the star, while the south-western jet exhibits helical structure and is observed all the way from the stellar image to  $\sim 16''$  or the edge of the ring nebula, between P.A.s of  $208^{\circ}$  and  $230^{\circ}$ . Nota et al. also detected a string of knotlike features extending from the far side of the SW jet in a northerly direction, at P.A.s of  $240^{\circ}$ ,  $255^{\circ}$ ,  $278^{\circ}$ ,  $300^{\circ}$ , respectively. The morphological features associated with the jet are mainly reflection nebulosities, areas of dust that scatter stellar radiation toward the observer, while the elliptical ring nebula is primarily an H II region (see Nota et al. 1992).

What is the origin of the axisymmetric structures seen in the circumstellar environment of AG Car? In this paper we present and discuss observations of the linear polarization of AG Car as a function of wavelength and time, and discuss implications for the stellar wind geometry at distances much closer to the star than have previously been probed.

## 2. OBSERVATIONS

The observations reported in this paper were obtained with the half-wave, CCD polarimeter of the 3.9 m Anglo-Australian Telescope (AAT). Typical observation and reduction steps were described in Schulte-Ladbeck et al. (1993). A double-decker is used to record the star and sky spectra simulta-

neously; the separation of the two apertures is  $\sim 25''$ , and the height of the apertures is  $2''.7$ . The aperture width is adjustable and was different for different epochs. At least four sets of observations of AG Car were obtained at each epoch with the sky and star apertures reversed twice. Each of these four data sets comprises 16 spectra, the star and sky spectra taken in the ordinary and extraordinary beams and at four different positions of the half-wave plate. The mean instrumental polarization over the entire spectral range was smaller than 0.1% on all occasions. There are several instrumental effects that introduce a small amplitude dependence of the polarization which we did not succeed in removing completely (see, e.g., Schulte-Ladbeck et al. 1993). The high-resolution data sets revealed a low-frequency periodic "ripple" with an amplitude of 0.1% in the data, which is probably introduced by the half-wave plate. Observational errors given in this paper are based on photon-counting statistics, because they can be related to the significance of a spectral feature in the polarization data. The temporal variation of the polarization,  $\sim 1.2\%$ , is highly significant even if we assume that there is a systematic error of 0.1% polarization in the absolute calibration of our data.

The first observation was taken on 1991 June 22 through a  $4''$  slit and covers a wavelength range from 3970 to 6920 Å at a calculated resolution of 14 Å (FWHM). The spectrum is displayed in Figure 1. The data were affected by an intermittent CCD-controller problem uncorrectable by data processing (see AAO Newsletter No. 60). This did not impair the spectroscopy apart from lowering the signal-to-noise ratio, but it introduced a random systematic error into the polarimetry. Even though the polarization data seem suspect, we can deduce some results. First, the polarization in one data set of the AG Car observations did not display the signatures of the CCD-controller problem. The mean polarization over the entire spectral range was  $P = 1.77 (\pm 0.01)\%$  at a position angle P.A. =  $140^{\circ}$ ; we will use this data point in the discussion of the time-dependence of the polarization. Second, we also notice in all four data sets a decrease of the percentage polarization at  $\text{H}\alpha$  and a net increase of the PA over the profile with respect to the continuum; and we take this to indicate that intrinsic polarization was present in AG Car at this epoch. We stress that subsequent observing runs were not affected by the CCD-controller problem.

The second observation of AG Car was acquired on 1991 November 27 through a  $2''.7$  slit. The observations cover a wavelength region from 4120 to 6870 Å, at an expected resolution of  $\sim 9 \text{ Å}$  (FWHM). Since the seeing improved to  $\sim 1''$  during the AG Car observation, the actual resolution of the data is slightly better. The reduced data of our second AG Car observation are displayed in Figure 2. The polarization data were binned to a constant error of 0.07% polarization, and thus exhibit a spectral resolution which is dependent on the recorded counts. We are confident that the polarization variations across the wings of the  $\text{H}\alpha$  line reported below are

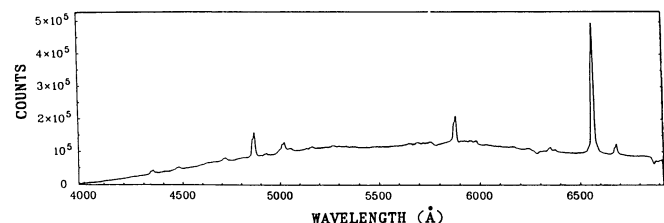


FIG. 1.—Spectrum of AG Car on 1991 June 22

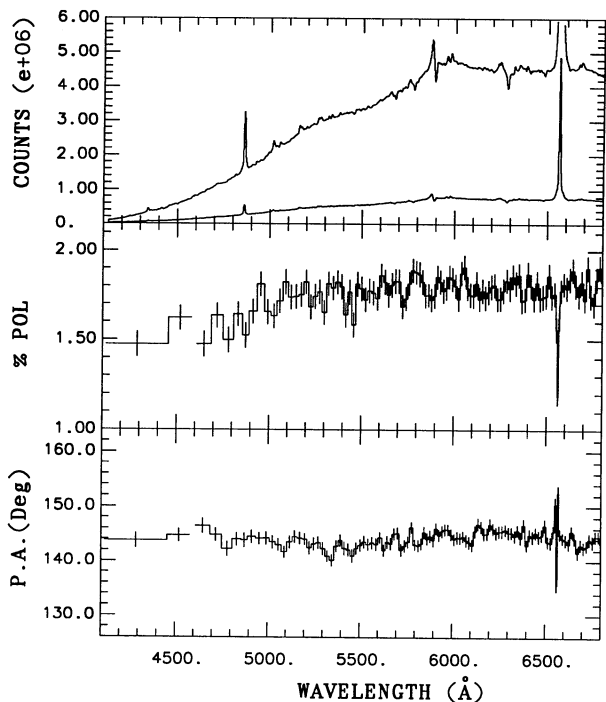


FIG. 2.—Spectrum and polarization of AG Car on 1991 November 27. The axes are plotted as counts, percentage polarization, and position-angle against wavelength. The counts spectrum was overplotted at a magnification of 6 so as to bring out the weaker emission lines. The presence of He I  $\lambda$ 5876 and absence of He II  $\lambda$ 4686 indicates that AG Car was a hot B-type star at the time. Polarization data were binned at a constant error of 0.07%, thus the resolution of the polarization spectra is dependent on the recorded counts. A very small section of the spectrum near 4600 Å was removed due to the likelihood that it was contaminated by a cosmic-ray hit on one of the spectra.

not an artifact of misalignment between the individual spectra, as great care was taken in the determination of a two-dimensional wavelength calibration.

The third observation was secured on 1992 March 15 through a 1.9" wide aperture. It covers the spectral range from 6250 to 6880 Å at a spectral resolution of 1.4 Å (FWHM). A two-dimensional wavelength calibration was employed. The polarimetric data were reduced using both the TSP software package available from the AAT, and software developed independently by two of us (Harries & Howarth). The observations are displayed in Figure 3; a binning of 0.03% was used.

The fourth observation was gathered on 1993 February 12 in a 1" aperture. This data set covers the spectral region from 3610 to 7060 Å, with a 6.5 Å (FWHM) resolution. The reduction steps applied were the same as those for the second observation. We present the observations in Figure 4 with a 0.03% binning of the polarimetric data.

Figure 5 shows a light curve of AG Car (S. Shore 1993, private communication). The arrows indicate how our observations were placed with respect to the general increase in visual brightness as well as some apparent short-term light variations of AG Car. Because of observational errors, however, there is some uncertainty about the validity of some of these short-term variations (C. Leitherer 1993, private communication).

### 3. THE SPECTRUM

The emission-line spectrum of AG Car underwent marked changes between 1991 June and November. Most notably, in

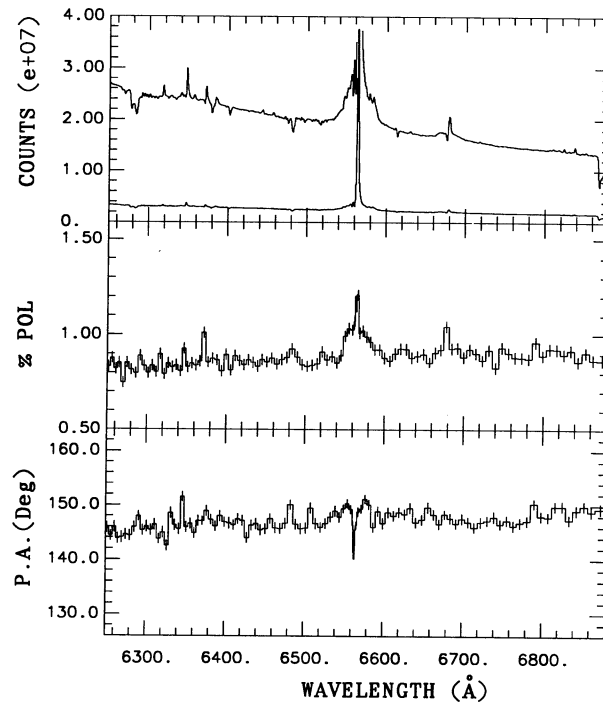


FIG. 3.—Spectrum of the flux, %P and P.A. on 1992 March 15. The polarization was binned to 0.03%.

our June spectrum the emission lines appeared to be double-peaked with the red peak being stronger than the blue peak. The strongest emission lines were the Balmer lines, Fe II (42) lines, and He I  $\lambda$ 5876, 6678 emissions, while the lines of He I  $\lambda$ 4471 and Si II (2)  $\lambda$ 6347 were weaker and He II  $\lambda$ 4686 was not apparent. The H $\alpha$  line clearly displayed broad line wings.

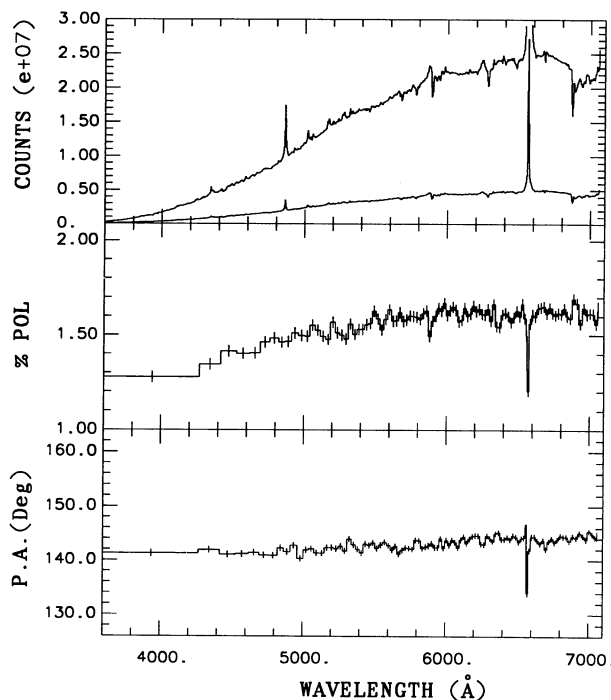


FIG. 4.—Spectrum of the flux, %P and P.A. on 1993 February 12. The polarization was binned to 0.03%.

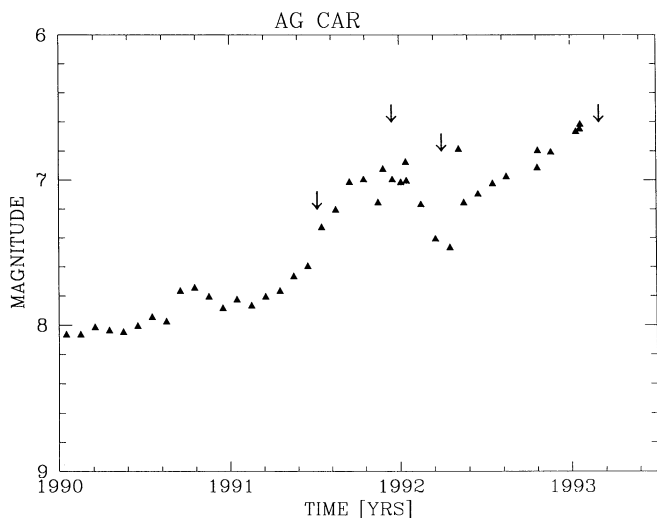


FIG. 5.— $V$  light curve of AG Car. The arrows indicate when the AAT spectropolarimetry data were obtained.

In November, all of the lines were single-peaked to within the spectral resolution. The He I spectrum appeared to have become weaker, the Na I D-lines blend could be distinguished from He I  $\lambda 5876$ , and He I  $\lambda 4471$  was absent. The region around  $5300 \text{ \AA}$ , which did not show many lines in June, displayed a wealth of weak emission features in November, attributable to numerous Fe II and [Fe II] lines. Both the  $H\alpha$  and  $H\beta$  profiles exhibit broad line wings. He II  $\lambda 4686$  was truant again.

The  $H\alpha$  profile of the high-resolution observation in 1992 March displays a narrow core of emission with the rise to line peak on the blue side steeper than the decline on the red side. The extended line wings can be traced to the same distance from line center as in our November 27 observation. The FWZI of the wings corresponds to a velocity of  $\sim 4100 \text{ km s}^{-1}$ . We note that He I  $\lambda 6678$  showed a P-Cygni absorption and also very broad line wings. Other emission lines in this spectrogram are identified with N II (2, 31, 41, 46), Si II (2), C II (2), Al II (2) and [N II].

The spectrum of 1993 February is again of low resolution. Compared with that of 1991 November, more weak lines are noticeable in the 1993 February spectrum. He I  $\lambda 5876$  and He I  $\lambda 6678$  (which looks as if only the wings and the absorption were present) were weaker, and Si II  $\lambda 6347$ , He I  $\lambda 4471$  and He II  $\lambda 4686$  were absent.

Measurements of the  $H\alpha$  equivalent width, derived from a straight summation of the counts under the line profiles including the line wings, are given in Table 1 for the last three epochs. The measurements show that the  $H\alpha$  equivalent width has been decreasing in the rise to maximum.

In summary, our spectroscopic data suggest that by late

TABLE 1  
MEASUREMENTS OF THE  
 $H\alpha$  EQUIVALENT WIDTH

UT Date	JD 2,440,000 +	EW( $H\alpha$ ) ( $\text{\AA}$ )
1991 Nov 27 .....	8588.2236	-67
1992 Mar 15 .....	8697.1757	-57
1993 Feb 12 .....	9031.1236	-50

1991 AG Car had evolved from a slash star to a B-type star. This is the typical trend of evolution toward lower temperature which marks an LBV excursion in the HR diagram toward the Humphreys-Davidson limit. The observed variations in visual brightness and accompanying changes in the optical spectrum thus indicate a new maximum in AG Car.

#### 4. THE POLARIZATION

##### 4.1. Observed Polarization

Figures 2–4 clearly show a change of polarization associated with the  $H\alpha$  emission line. Observed polarization generally consists of two components: the interstellar polarization (ISP) on the line of sight, and the intrinsic polarization of the star/envelope. The  $H\alpha$  emission comes from the stellar wind, and thus the observed polarization changes at  $H\alpha$  require the presence of intrinsic polarization in AG Car. The change of polarization at  $H\alpha$  is seen in all of our data sets, and we thus find that an intrinsic polarization component was present in all four of our observations.

In Figures 6–8 we have zoomed in on the observations in a narrow wavelength region centered on the  $H\alpha$  line. We chose to bin the polarimetric data in a way that brings out best the shapes of the features. The % $P$  in Figure 6 shows a broad trough coincident with the line core, while the P.A. is observed to oscillate above, below, and above the continuum with increasing wavelength. In the subsequent observation (Fig. 7), the % $P$  increases above the continuum level across the line. The line shows two % $P$  components, one broad and extended, one narrow and peaked. The P.A. oscillation across the profile is similar to that observed before. The % $P$  during our last

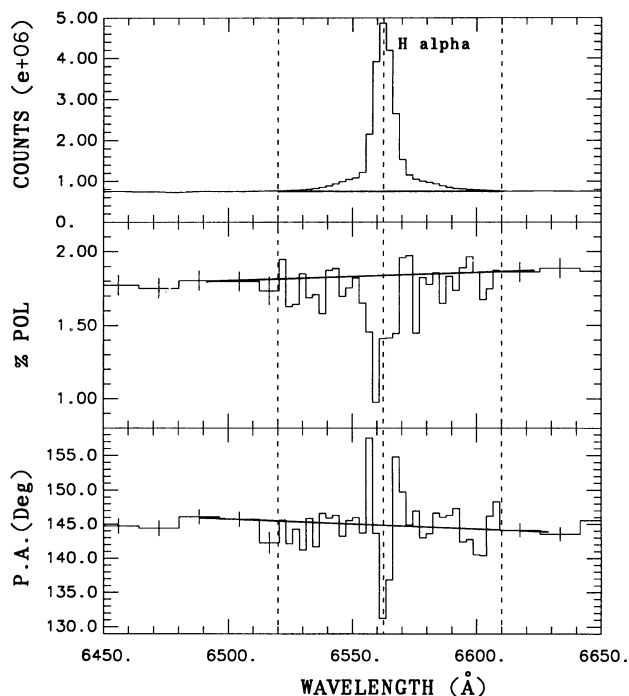


FIG. 6.—Zoom in on the  $H\alpha$  line of AG Car on 1991 November 27. Notice the very extended line wings. Polarization across the extended line wings is shown pixel-by-pixel so as to illustrate the observed signal-to-noise, while that of the continuum was binned to 0.07%. Dashed lines were drawn at line center and where the extended line wings meet the continuum; the solid lines indicate the location of the continuum. Note the changes in the position angle across the line wings.



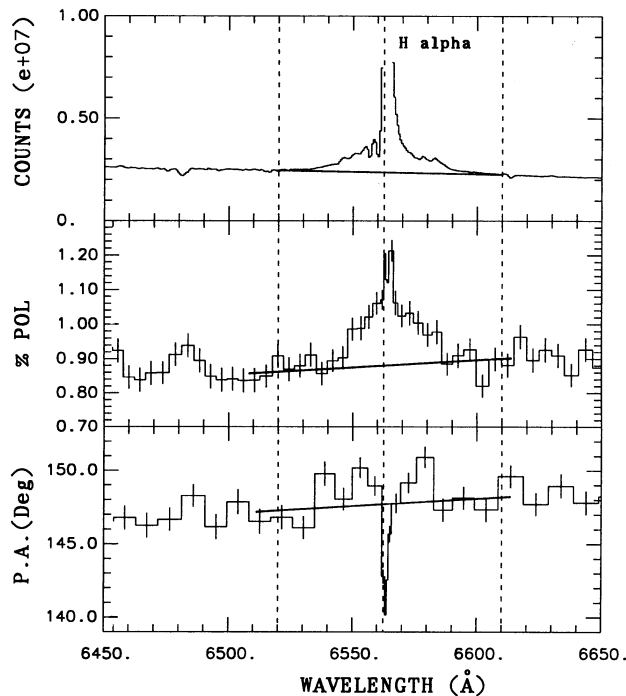


FIG. 7.—Zoom in on the H $\alpha$  line of AG Car on 1992 March 15. Notice the polarization changes associated with the extended line wings of H $\alpha$ , and the different polarization in the line core with respect to the line wings, and also the difference in the % $P$  across the line core with respect to the changes observed on 1991 November 27 and 1993 February 12.

observation (Fig. 8) again decreases across the line, while the P.A. shows a concomitant decrease but then remains below the continuum value in the red line wing.

At first glance, the behavior of the % $P$  across the line appears puzzling. The emission line is created by recombina-

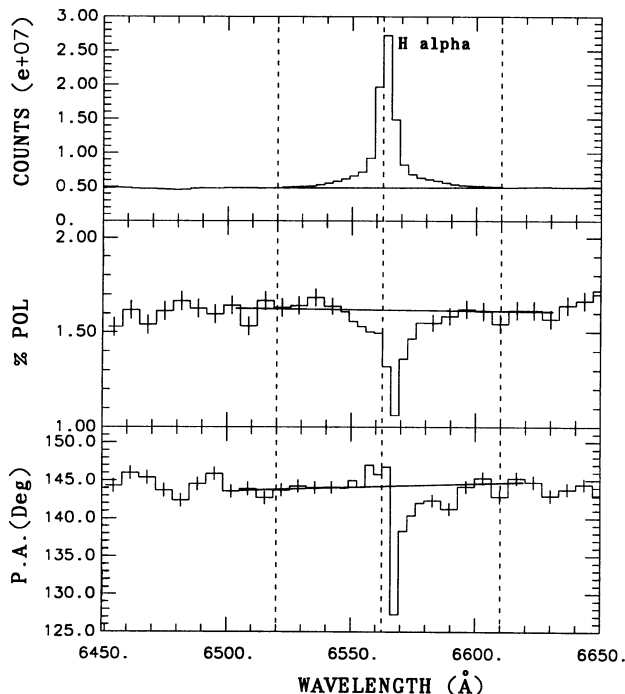


FIG. 8.—Zoom in on the H $\alpha$  line of AG Car on 1993 February 12

tion hence unpolarized. The polarization at the line wavelength (continuum plus line) is thus expected to decrease across H $\alpha$ , because the unpolarized emission dilutes the polarized continuum radiation. But recall that our observations contain an unknown amount of ISP. Hence the fact that the observed polarization at H $\alpha$  is sometimes above, and sometimes below, the observed continuum polarization does not exclude the possibility that the *intrinsic* polarization decreased across the line at all times. The observed polarization at the line wavelength does indicate that the intrinsic continuum polarization of AG Car varies with time in such a fashion that it sometimes adds to, and sometimes subtracts from, the ISP.

As noted in § 3, all of our spectra exhibit broad wings of the H $\alpha$  line. Our observation that the polarization in the line wings differs from that in the continuum verifies that the line wings are caused by scattering. In order for line photons to scatter at electrons, the electron-scattering optical depth in the wind of AG Car must be substantial even to the line-forming region and, for this polarization to be detectable, the asymmetry of the wind must also extend out to several stellar radii. The P.A. in the wings is different from that in either the continuum or the line center, but the blue and red wing of a given profile appear to have the same P.A. in our 1991 and 1992 data sets. Together, these % $P$  changes and P.A. rotations describe hook-shaped tracks in  $Q$ - $U$  space across the profiles, rather than linear tracks (expected for dilution alone), or loops (predicted from single scattering of line photons in a rotating, Keplerian disk which is not viewed exactly edge-on by the observer; cf. Wood, Brown, & Fox 1993). According to the models produced by Wood et al., only a rotating *and* expanding disk will result in polarization profiles that would describe hook-shaped tracks in  $Q$ - $U$  space.

We determined the polarizations in the line cores with the continuum polarizations subtracted. The continuum levels were set by linear interpolation between the polarization in spectral regions to the blue and red of the line. The results for H $\alpha$  are shown in Figure 9. Notice how well the line polarizations at all epochs agree to within the errors. In Figure 9 we drew lines from the point representing the tip of the continuum polarization vector to that of the line polarization for each epoch; these are the vector differences which we also refer to as the continuum-to-line vectors. They are indicators of the change in the intrinsic polarization of AG Car. The continuum-to-line vectors on November 27 and February 12 showed an intrinsic position angle of  $\sim 145^\circ \pm 3^\circ$ , which is very similar to the position angle of the observed continuum polarizations. On November 27 and February 12, we measured the polarization in H $\beta$  and He I  $\lambda 5876$  as well. These data have much larger observational errors so we do not display them in Figure 9 for the sake of clarity. The polarizations in these lines do agree within the errors with the H $\alpha$  measurements. On March 15 the polarization in H $\alpha$  has not changed compared to November 27 or February 12, but the polarization in the continuum is very different. The continuum-to-line vector displays a P.A. of  $43^\circ \pm 1^\circ$ . The continuum polarization is located on the other side of the line polarization compared with the data sets described above. That is to say, the position angle of the continuum polarization has flipped by almost  $180^\circ$  in  $Q$ - $U$  space, or almost  $90^\circ$  on the plane of the sky.

Our observations indicate that the continuum polarization of AG Car is variable as a function of time. In Figure 10 we plotted observations of AG Car taken at different times in selected line-free continuum bands, our data point from June

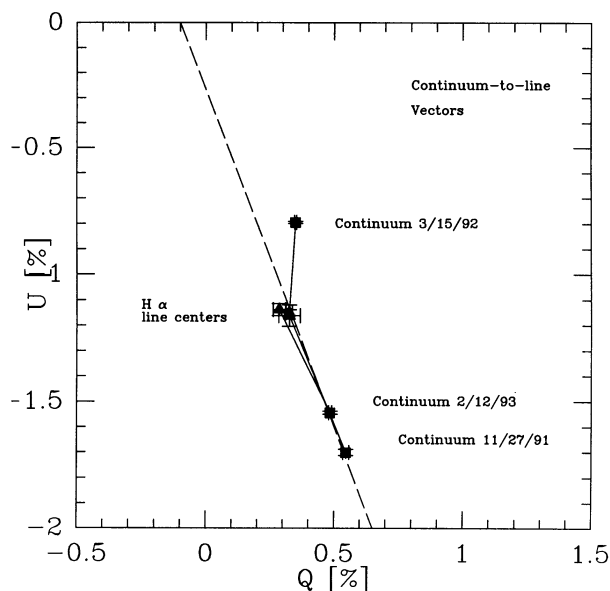


FIG. 9.— $Q$ - $U$  diagram showing the continuum-to-line vectors for  $H\alpha$ . Notice how well the polarization in the line agrees for different epochs, while the polarization in the underlying continuum is quite variable. The dashed line indicates the direction of the intrinsic polarization inferred from the continuum-to-line vectors.

22, and the multiple-epoch  $UBV$  polarimetry of Serkowski (1970).<sup>2</sup>

More than 20 years ago Serkowski observed AG Car 8 times over a period of 511 days (1968 January to 1969 June). He had measured its linear polarization in the  $U$ ,  $B$ , and  $V$  filters and also recorded its  $V$  magnitude. AG Car had a visual magnitude of 6.8 mag in early 1968; by mid-1969, it had dropped to  $\sim 7.5$  mag. Comparison with the light curve of Mayall (1969) shows that AG Car was in the second half of a maximum to which it had begun to rise in late 1963. We converted Serkowski's polarization data from magnitude into  $\%P$  using the approximation given in Appenzeller (1966). The error for the Serkowski data in Figure 10 is 0.06% and is that which we consider a typical  $1\sigma$  error for these observations following the mean error estimates of Serkowski (1968). Whenever multi-color data are available, they show a trend of increasing polarization from  $U$  to  $V$ .

It is interesting to note that Serkowski made a test using different observing apertures during the first night of observation. He measured the polarization through a  $5''$  aperture and then through a  $25''$  one, and did not find them to differ significantly. This indicates that the contribution of polarized scattered light from the nebula to these measurements is negligible. Serkowski had already noticed that the polarization of AG Car was variable. In Serkowski's observations, the polarization was

<sup>2</sup> Barbier & Swings (1981) also measured the polarization of AG Car in the  $UBV$  filters, in 1980 March. The lightcurve of Hutsemekers & Kohoutek (1988) shows that AG Car had just risen sharply to an extremely bright visual maximum of about 6 mag. Individual error bars were not provided by Barbier & Swings. Also, the authors measured the polarization of surrounding field stars to determine the ISP and then they removed it, but they did not publish it. The data are presumed to represent the intrinsic polarization, of 0.5%–0.8%. Due to the uncertainties involved in the removal of ISP, we did not consider these data in our paper. Recently Leitherer et al. (1992a) reported the detection of polarization in AG Car in the ultraviolet,  $1\% \pm 0.2\%$  between 2900 and 3300 Å, with the *HST*, presumably on 1991 November 19. However, they did not provide the P.A. of the observation, so that we could not include their data in our  $Q$ - $U$  diagrams.

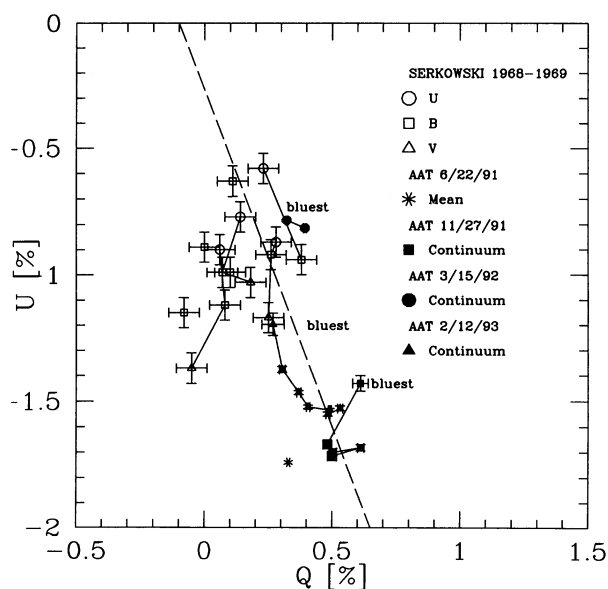


FIG. 10.—Polarization data of AG Car taken on 12 different occasions over more than 20 years. Observations utilizing different filters but obtained during the same night were connected. The dashed line shows the P.A. that best describes the average location of the data,  $145^\circ$ . The temporal variations follow along the same P.A. as the continuum-to-line vectors of Fig. 8.

typically around 1%, with variations of  $\pm 0.4\%$ . The variability in our AAT data and in Serkowski's data suggests that the polarization undergoes changes on timescales that are shorter than an LBV cycle. Like our's, the observations of Serkowski were spaced out by months, but on one occasion, two data sets were obtained only 4 days apart and the variation was  $3\sigma$ .

Our first two AAT data sets display a much larger average polarization than Serkowski ever observed, 1.7%–1.8%, while the third set agrees with Serkowski's polarizations, and the fourth spans the range in between these extremes. This latter data set displays a marked wavelength dependence of the line-free continuum polarization (cf. Fig. 10), with a P.A. along that which we interpret as the intrinsic P.A. We notice that the highest observed polarizations coincide with times when the star was faint (cf. Fig. 5). In Serkowski's data set, higher observed polarizations also correspond to lower visual brightness. The total range of the percentage polarization variations is  $\sim 1.2\%$ . The range of P.A.s is  $\sim 20^\circ$ .

The average P.A. of the temporal polarization variations is the same as that measured from the  $H\alpha$  continuum-to-line-center vectors, and the color dependence of line-free continuum observations on February 12. The data can be interpreted to indicate the existence of a preferred symmetry axis in the distribution of scatterers, at  $\sim 145^\circ \pm \sim 10^\circ$  (or at  $55^\circ$ ).<sup>3</sup> However, there remains the possibility that this is merely an artifact of the limited temporal sampling of the polarization data, the impression of a preferred position angle having arisen by chance. Obviously, future polarimetric measurements of AG Car are highly desirable to study whether polarizations in

<sup>3</sup> The axis of symmetry has a  $90^\circ$  ambiguity for the following reasons: (1) The intrinsic P.A. may be either  $145^\circ$  or  $55^\circ$  since it depends on where the ISP meets the distribution of observed polarizations. This ambiguity is removed once the ISP is known. (2) The interpretation of the P.A. then requires an assumption of whether the source has a prolate or oblate density structure. In the optically thin case the P.A. of an oblate envelope is parallel to the axis of symmetry, but for the prolate case the symmetry axis is at  $90^\circ$  to the P.A. (Brown & McLean 1977).

directions other than from about  $135^\circ$  to  $155^\circ$  occur at some times.

Summarily, without knowledge of the interstellar polarization, we can establish that the wind of AG Car is variable most likely owing to electron scattering optical depth fluctuations that occur in maximum state (Serkowski's data) as well in the rise to it (our data). If we believe the mean errors of Serkowski then a  $3\sigma$  variation was observed once in two data sets which were taken only 4 days apart, and this suggests that the scattering material resides close to the star, as expected (Rudy 1978; Cassinelli, Nordsieck, & Murison 1987). In addition, the polarization variations with wavelength across the  $H\alpha$  line profile are in agreement with the systematic mass motions of a rotating, expanding, flattened stellar envelope. The matter ejections appear to take place along a preferred axis near  $145^\circ$  (or  $55^\circ$ ) about which there is some scatter. This is our second piece of evidence for the presence of a latitude-dependent, global wind structure. If the line-core polarization of  $H\alpha$  is an indicator of the ISP, then the intrinsic continuum polarization has shown a rotation by  $\sim 90^\circ$  on the sky as a function of time, indicating that polarization in one quadrant of the wind can at times be dominated by that of an adjacent quadrant. Since the  $Q$ - $U$  time variation lies along a linear track that extrapolates back to the origin of the  $Q$ - $U$  diagram, the intrinsic polarization and the ISP must be nearly colinear or at  $90^\circ$  with respect to one another.

#### 4.2. Intrinsic Polarization

The intrinsic polarization is strongly dependent upon the adopted parameters of the ISP. Therefore, results derived in this section are less secure than those reported above. An excellent description of the methods available to separate ISP and intrinsic polarization in early-type emission-line stars can be found in McLean & Clarke (1979). Below we discuss their application to AG Car.

We first attempted to narrow down the choice of ISP using the field-star method. The results are given below and are not conclusive in their own right. The field-star method is based on measurements of the polarization of stars on nearly the same sightline as the intrinsically polarized star under scrutiny. Ideally, we would have liked to have polarization measurements of stars at the same distance as AG Car, that is, the stars from the sample of Hoekzema, Lamers, & van Genderen (1992) that were used to derive the interstellar reddening and new distance to AG Car. However, none of those stars has had its polarization published in the literature. We have not attempted to obtain new measurements because this would constitute a major observing run. Instead we used the polarization data in the WUPPOL catalog, a database of polarization measurements compiled by M. R. Meade (1993, private communication). Figure 11 shows the polarization of field stars within a circle of  $2^\circ$  radius on the sky around AG Car. This sample excludes data of stars with spectral types which would suggest that they might be intrinsically polarized. We split the sample into two distance bins containing roughly the same number of measurements, with distance moduli  $< 12.5$  and  $\geq 12.5$  mag. According to its new distance, AG Car has a distance modulus of  $\sim 14$  mag. The ISP appears to be quite variable as a function of location, attaining values anywhere between a few tenths of a percent to 2% in amount, but is confined in P.A. to the third and the fourth quadrant of the  $Q$ - $U$  diagram. It is not possible to determine the ISP on the line-of-sight to AG Car with these data.

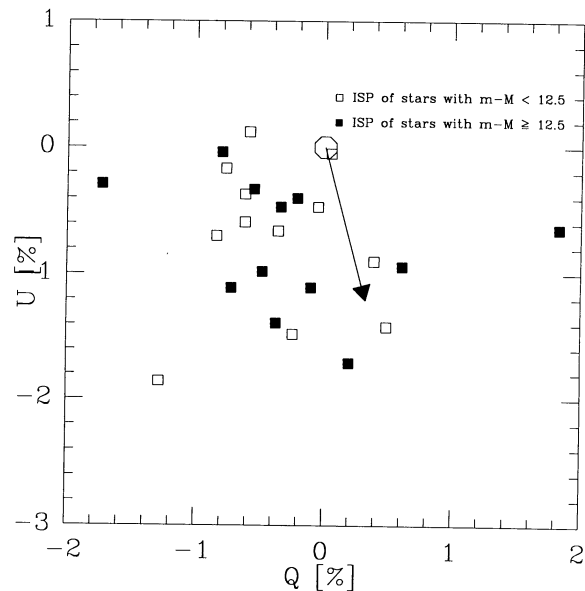


FIG. 11.— $Q$ - $U$  diagram of field stars located within a circle of  $2^\circ$  radius around the position of AG Car on the sky. Note the different scale of the  $Q$  and  $U$  axes compared to Figs. 8 and 9. The open octahedron shows the zero point of the diagram. The arrow indicates the ISP vector based on  $H\alpha$ .

The separation of ISP and intrinsic polarization was successfully performed using the  $H\alpha$  polarization in the LBVs P Cygni (Taylor et al. 1991) and R127 (Schulte-Ladbeck et al. 1992b). In AG Car, however, the situation may not be as simple because of the obvious underlying line-wing polarization. We nevertheless assumed that the polarization in the  $H\alpha$  line core (with the continuum removed) represents the ISP at  $6562 \text{ \AA}$ . This seems justified because the line is very strong at line center where the direct, unscattered  $H\alpha$  emission dominates over the small, scattered component of the underlying line wing. Very strong support for the validity of our assumption comes from the fact that the polarization in the line at line center has not varied as a function of time (see Fig. 9), whereas the continuum polarization has varied largely. The three independent measurements were used to find the following arithmetic means and their standard deviations:  $Q = 0.31\% \pm 0.02\%$ ,  $U = -1.15\% \pm 0.01\%$ . The arrow drawn in Figure 11 indicates the ISP vector based on the  $H\alpha$  line polarization. It shows that the polarizations of field stars on the AG Car sightline are not inconsistent with our conjecture.

In order to subtract the ISP, we have to make an additional assumption about the wavelength at which its maximum occurs. The map of  $\lambda_{\text{max}}$  versus galactic coordinates by Serkowski et al. (1975) indicates a value in the vicinity of AG Car of  $5200 \text{ \AA} \leq \lambda_{\text{max}} \leq 5400 \text{ \AA}$ . We first adopted  $\lambda_{\text{max}} = 5300 \text{ \AA}$  for AG Car, which corresponds to  $R_V \approx 3$ . After subtracting an ISP with this value for  $\lambda_{\text{max}}$ , our data showed strong and systematic wavelength dependencies of both the %P and P.A. In particular, the data sets having large wavelength coverage showed an increase in the intrinsic polarization with increasing wavelength. Such behavior is difficult to explain and is not the expected spectral form of any model predictions involving electron scattering and competing hydrogen absorption.

We therefore also abandoned the field-star-based value of  $\lambda_{\text{max}}$ . Instead, we used the AG Car data set with the most wavelength coverage to conduct a parameter study of  $\lambda_{\text{max}}$  on



the actual sightline. We asked whether a flat spectrum of the intrinsic % $P$  and P.A. could be achieved with any reasonable value of  $\lambda_{\max}$ . The program that we used is based on the Wilking, Lebofsky, & Rieke (1982) version of the Serkowski law (for an update, see Whittet et al. 1992). Our study showed that at a  $\lambda_{\max}$  of 6900 Å, both the intrinsic % $P$  and P.A. become flat as a function of wavelength with variations in  $P$  of 0.05%, and variations in P.A. of 12° across the entire spectral range. Moreover, when we subtracted the corresponding polarization of 1.2% at a P.A. of 142°5 from the other data sets, these also showed constant intrinsic % $P$  and P.A. versus wavelength. The value for  $\lambda_{\max}$  thus derived implies  $R_V \approx 3.9$  toward AG Car. A higher  $R_V$  value would increase the luminosity of AG Car and make it even more unlikely that it has passed through a red supergiant phase.

To the best of our knowledge, there is no work which addresses the value of  $R_V$  on the AG Car sightline. The interstellar extinction in the Carina region was reviewed by Hillier & Allen (1992). Most authors derive large values of  $R_V$  in the Carina nebula and several clusters in the vicinity. However, AG Car is not located in the Carina nebula or any of the clusters that have been studied in the literature. Hoekzema et al. (1992) determined  $E(B-V) = 0.63$  for AG Car, which translates into an upper limit of  $P \leq 5.67\%$  for the ISP. The smallest values of  $E(B-V)$  on the sightline appears to be around 0.13, yielding a lowest upper limit of  $P \leq 1.17\%$ .

The final ISP parameters deduced are:  $P_{\max} = 1.2\%$ ,  $\lambda_{\max} = 6900$  Å, P.A. = 142°5. These parameters appear to be reasonable and can only be improved when data covering a larger wavelength interval and/or observations of very nearby stars to AG Car become available.

By default, the spectra of the intrinsic polarization show decreasing % $P$  across H $\alpha$  at all epochs, and the overall slope of the intrinsic polarization at any epoch is flat. In Figure 12 we

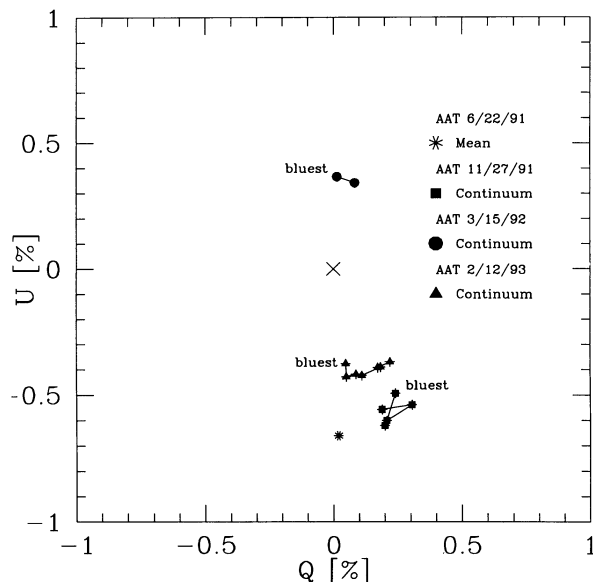


FIG. 12.— $Q$ - $U$  diagram of the intrinsic polarizations of the AAT data (the Serkowski data would be located just to the left of the 1992 March 15 observation). The origin of the  $Q$ - $U$  diagram is marked with an X, and the scale is the same as that of Figs. 8 and 9. The polarizations at different times are found to be located on opposite sides of the origin, and along an axis that goes through the origin. This corresponds to a variation by  $\sim 90^\circ$  on the plane of the sky. Notice the reduced wavelength dependence in the data as compared to Fig. 10.

plot the intrinsic polarizations for the AAT observations in the  $Q$ - $U$  plane, using the same scale as in Figure 10. Since the ISP that we derived is located between the March 15 (and the Serkowski) observations and the AAT observations at the other epochs, the former and the latter data sets are now located on opposite sides of the origin of the  $Q$ - $U$  diagram. Such a flip implies that the electric vector has rotated by  $90^\circ$  in the plane of the sky.

Two simple mechanisms can be envisaged which might cause the intrinsic polarization to flip by  $90^\circ$ . First the wind of AG Car might be represented by two major flows, each described by its own mass-loss rate and terminal velocity. In the simplest scenario one of these flows is in the equatorial plane, while the other is a polar flow. The resulting polarization of such a two-component wind has recently been calculated by Taylor & Cassinelli (1992). The sign of the resultant polarization is then determined by the dominant flow. With this mechanism, the flip in polarization requires a change in the mass-loss rate (wind density) in at least one direction, and thus a change in the asymmetry of the wind.

An alternative explanation is to assume that multiple scattering effects are important. For an equatorial flow the polarization is parallel to the symmetry axis provided the flow is optically thin. At sufficiently high optical depth, however, the polarization may reverse sign (Hillier 1994). In this scenario, only a change in the optical depth of the wind (due to mass-loss variations or changes in the stellar radius) is required.

Test calculations show that this premise is not unreasonable. In particular we have performed polarization calculations for a model with  $R_* = 75 R_\odot$ ,  $L = 10^6 L_\odot$ ,  $V_\infty = 200 \text{ km s}^{-1}$ ,  $\dot{M} = 2.5 \times 10^{-5} M_\odot \text{ yr}^{-1}$ , and  $N_{\text{H}}/N_{\text{He}} = 4$ , parameters that are typical of LBV-type stars. A very slow velocity law (with  $\beta = 6$ ) was used, although  $\beta = 1$  to 3 is probably more reasonable. These calculations show that mass-loss variations of a factor of 2 (about the mean mass-loss rate) can indeed give rise to a flip in the sign of the observed polarization. For these calculations the mass-loss rate was assumed to have an angular variation of the form  $1 - 0.5 \cos^2 \Theta$  where  $\Theta$  is the polar angle.

In a subsequent paper we intend to investigate the polarization variability by considering models specifically designed to match the observed spectrum of AG Car. An important tool for diagnosing the polarization flips will come from examining the polarization behavior with wavelength.

## 5. DISCUSSION

We have obtained optical spectropolarimetry of AG Car on the rise to a new maximum and compared our results with polarimetric data from the literature.

The polarization changes across the extended wings of the H $\alpha$  emission line. Broad line wings of the H $\alpha$  profile were first noted in the spectrum of the LBV P Cygni and interpreted with line broadening by scattering at electrons having high thermal velocities by Bernat & Lambert (1978). Bernat & Lambert suggested that electron scattering should also give rise to a change in polarization across the line profile. Wolf & Stahl (1982) reported extended wings on the Balmer lines of AG Car with a total width of  $\sim 2000 \text{ km s}^{-1}$ . In contrast, the mean expansion velocity of the envelope was determined to be only  $\sim 95 \text{ km s}^{-1}$  from the P-Cygni absorption components of numerous spectral lines. This made it very unlikely that the extended wings of the Balmer lines could be explained in terms of a shell expanding at high velocity. Wolf & Stahl instead attributed the extended line wings of AG Car to electron scat-



tering in a dense stellar wind and derived  $\tau_e = 0.8$  and  $T_e = 9000$  K using simplified profile fitting. Hiller, McGreger, & Hyland (1988), and Hiller (1991) have made detailed calculations for electron-scattering wings in LBVs and showed that the results are qualitatively consistent with those observed.

The interpretation of the extended Balmer-line wings in LBVs with electron scattering was subsequently challenged by Hubeny & Leitherer (1989). They showed that extended wings might also occur as a result of non-LTE effects in a low-gravity atmosphere. Our detection of polarization in the H $\alpha$  line wings of AG Car confirms the identification of its extended line wings with electron scattering.

The polarization of AG Car is variable on timescales of days to months. The polarimetric variations observed in AG Car are reminiscent of those observed in other LBVs. In R127 (observed in maximum) and P Cygni (observed in minimum) the polarizations varied by about half a percent (Schulte-Ladbeck et al. 1993; Taylor et al. 1991). Taylor et al. found that polarization variations by this amount correspond to electron column density changes in the "plume" model by about an order of magnitude. In AG Car, the amplitude of the intrinsic variations is observed to be about twice as large as those of R127 and P Cyg.

The short-term variations are probably due to an ever-present level of activity in LBV winds, for example, electron scattering optical depth fluctuations that are not massive enough to produce LBV-cycle-type brightness variations but that manifest themselves in polarization variations, photometric microvariations, and multiple P-Cygni absorption or emission components of line profiles (see Hutsemékers & Kohoutek 1988). Note that the presence of polarization variations rules out globally spherical density fluctuations such as the formation or ejection of dense, spherical shells. The microvariations and other short-term phenomena are commonly believed to involve pulsations of the stellar photosphere (Lamers 1987).

The wavelength-time dependence of the polarization indicates that the stellar wind of AG Car has a symmetry axis along a P.A. of  $\sim 145^\circ$  (or perpendicular to it). We wish to emphasize that the derived P.A. is independent of any assumption concerning the ISP. Comparing the preferred P.A. with the morphology of the resolved features around AG Car, we note that the P.A. of the *polarization is nearly parallel to the major axis of the ring nebula*, which has a P.A. of  $\sim 135^\circ$ , and it is almost perpendicular to the jet, along P.A.s of  $\sim 35^\circ$  and  $\sim 225^\circ$ . This point is illustrated in Figure 13. Our observations can thus be interpreted to indicate that the asymmetries seen in the circumstellar environment of AG Car *are already present within the stellar wind* at a few stellar radii from the photosphere.

Nota et al. proposed three scenarios that could explain the resolved structures surrounding AG Car. First, a disk supported by rotation and a magnetic field could have formed in the equatorial plane of the star and could be focusing the stellar wind into a bipolar flow along the poles. The linear track in the  $Q$ - $U$  diagram of the polarization variations with time and the continuum-to-line vectors indicate that the stellar wind is axisymmetric, although we cannot tell without detailed modeling whether  $145^\circ$  or  $55^\circ$  is the axis of symmetry. Second, the stellar wind could be spherically symmetric at the outstart, but might encounter an anisotropic density and pressure distribution in the surrounding interstellar medium as it expands to larger distances. This model is clearly ruled out by the mere

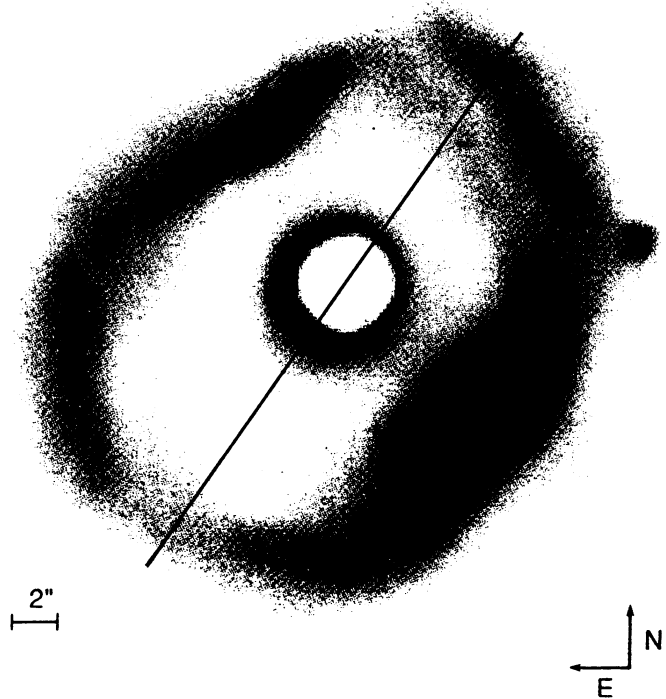


FIG. 13.—Coronagraphic image of the AG Car nebula in H $\alpha$  + [N II] courtesy of M. Clampin. The direction of the polarization vector is shown and is seen to be parallel to the major axis of the ring nebula.

presence of continuum polarization. Third, AG Car could be a binary system, and the outflow might be both regulated and channeled as a result of interaction with the companion. A much larger body of observations than currently in hand is needed to either prove or disprove the binary hypothesis using this particular observing technique. While the brightness variations of AG Car can be described as quasi-periodic, there are so far no claims of a single periodicity in either photometric or spectroscopic data sets. Consequently, the only support for the binary hypothesis is that it could explain the axisymmetric circumstellar features, but so could a latitude-dependent stellar wind.

We favor an axisymmetric wind model for AG Car. Apart from our polarimetric results, this picture is also supported by high-resolution spectroscopic data. Hutsemékers & Kohoutek proposed that differential rotation plus expansion of the stellar wind could account for the radial-velocity behavior of the emission subpeaks of the Balmer lines, as well as the double-peaked structure observed for the [Fe II] lines which originate at much larger radii.

The polarization of AG Car has only been monitored near or in the maximum state; it should be interesting to continue to observe it into the minimum state. Leitherer et al. (1992b) recently suggested that the mass-loss rate of AG Car is essentially the same in minimum and maximum, in contrast to other LBVs, which are known to display increased rates of mass loss during maximum. If the radius of AG Car increases during maximum as proposed by Leitherer et al., this implies that the wind density would be much lower at maximum than it is at minimum. Hence, further monitoring of the polarization into the minimum state, together with a model for the polarization, should provide tight constraints on the envelope geometry, and should lead to significant insights into the LBV variability mechanism.

The presence of an inhomogeneous and nonspherically symmetric wind has implications for the value of the mass-loss rate. Mass-loss rates are usually derived using the assumption of a spherical outflow. If the stellar wind is aspherical instead, the stellar mass-loss rates can in error by a factor of 2 or more, depending on the structural scale length ratios of the asymmetries (Schmid-Burgk 1982). Uncertainties in the mass-loss rate of even a factor of 2 would, however, have a pronounced effect on evolutionary models (Maeder 1990).

Stellar luminosities are based on the assumption that the observed flux arises from a spherical stellar disk. If the scattering optical depth in the wind is significant, the nonspherical geometry of the electrons will also result in a nonisotropic radiation field. This will have consequences for the stellar luminosity, and how it evolves with time. In a scattering-dominated photosphere, asphericity can cause a difference of up to 40% in luminosity compared to the spherical case (Höflich 1991). Since the bolometric luminosity derived is model dependent, it will take specific models of the envelope geometry before we can determine whether AG Car crosses the HR diagram at constant luminosity.

An axisymmetric wind could be produced by stellar rotation, or could be due to binarity. Sreenivasan & Wilson (1989) have proposed that rotation plays a significant role in the structure and evolution of massive stars in the upper left corner of the HR diagram. They find that many features of the upper HR diagram can be explained with stellar rotation, and that the required initial rotation velocities on the main sequence are not unrealistically high. In their model, an LBV wind has two components, the usual radiatively driven wind, and a wind supported by mechanical energy flux generated from the shear between the spun up stellar core and the envelope. They point out, as do Underhill & Fahey (1984) and Poe, Friend, & Cassinelli (1989), that rotation leads to a latitude-dependent mass loss, with an enhancement of the equatorial over the polar mass-loss rate. More recently, Bjorkman & Cassinelli (1993) have shown how rotation can significantly modify the wind geometry when the rotational velocity is comparable to the terminal velocity.

In analogy to models proposed for the formation of planetary nebulae, an axisymmetric, slow wind in an earlier evolutionary phase of AG Car might provide the "seed" for the formation of an axisymmetric shell during a later evolutionary phase in which the star developed a fast wind. We suggest that the faint, extended H $\alpha$  emission recently detected outside of the AG Car ring nebula might be the remnant of such a stellar wind from an earlier evolutionary phase. A dynamical model for the AG Car nebula based on the interaction of a young, hot stellar wind with an old, slow wind from an earlier, yellow-supergiant phase was recently presented by Robberto et al. (1993). We note that our data cannot provide additional information on the physical parameters of the LBV precursor, that is, whether it passed through a cool supergiant phase or not. The older, axisymmetric wind could as well have been shed during a blue-supergiant phase into which the presumed shell ejected during the LBV outburst, or any fast wind that occurred at a later evolutionary stage, expanded.

The observational data presented in this paper thus lead us to propose that the axisymmetric structures of the nebular features surrounding AG Car are a manifestation of the presence of an axisymmetric stellar wind that predates the formation of the AG Car ring nebula. Although the binary hypothesis cannot be ruled out on the basis of our data, we find

that a single, rotating central star can account for the observations in a satisfactory manner. We note that similarities exist to the B[e] star class as well as to other LBVs. In  $\eta$  Car, a disk close to the star has been inferred from echelle spectropolarimetry and spectroscopy of the axisymmetric Homunculus nebula (Warren-Smith et al. 1979; Hillier & Allen 1992; Hamann et al. 1994). Global wind asymmetries have been detected with polarimetry in R127, and this star also is surrounded by an axisymmetric nebula (Clampin et al. 1993b).

On the other hand, the wind of P Cyg appears to be globally spherical or only slightly flattened (Taylor et al. 1991). One possible explanation of this behavior might be that P Cyg is a single star, whereas the other LBVs harbor binary companions. Otherwise, if the phenomena that we see originate in single stars, we could postulate that all of the objects have flattened stellar winds, but that we view them under different inclination angles. We do not believe that the difference in P Cygni's polarimetric behavior is an inclination effect, that is, that it has a disk, but we view this star from above the pole. By analogy to Be stars we might expect that the polar wind is significantly faster than the equatorial wind. If this were so, P Cyg should have a higher terminal velocity than AG Car, whereas the reverse is true (cf. Smith, Crowther, & Prinja 1994).

Rather, we speculate that stars evolving off the main sequence with a spectrum of rotational velocities show latitude-dependent winds to varying degree, with slow rotators displaying spherical mass loss throughout their lives, and the very fast rotators evolving with equatorially enhanced stellar winds that later may account for the axisymmetry in their resolved nebulae. However, conservation of angular momentum requires that as stars evolve into supergiants they spin down; in mass-losing stars, angular momentum is lost by the star, and high rotation cannot be recovered in a later phase even if the stellar radius becomes smaller. A possible solution was pointed out by Maheswaran & Cassinelli (1994). It requires the large mass-loss episodes to occur along the polar axis of the star, which would not carry away angular momentum.

In order to test Maheswaran & Cassinelli's models for evolution of massive stars with rotation, it is important to establish observationally whether there are mass-ejections related to an LBV's approach to the Humphreys-Davidson limit, and if these occur in a polar wind. One of the possible interpretations of our data involves significant changes in the angular distribution of mass loss. If significant mass loss is associated with the maximum phase, and if it is in polar flows, a massive star might retain its angular momentum in the LBV phase and into the W-R stage (Maheswaran & Cassinelli 1994). This would allow us to make an evolutionary connection to W-R stars with significant polarization (Schulte-Ladbeck et al. 1990; Schulte-Ladbeck et al. 1992b), which might also be rapid rotators.

## 6. CONCLUSIONS

Observations of the linear polarizations of AG Car on the rise to maximum state can be interpreted with electron scattering in an axisymmetric, inhomogeneous, time-dependent stellar wind. The wings of the H $\alpha$  emission line are partially polarized, which provides direct observational support for their identification with electron scattering. We point out that the anisotropy of the wind may change the mass-loss rates derived using the assumption of a spherical flow, as well as the inferred stellar luminosity and its time dependence. The impor-

tance of these effects cannot be assessed without suitable models of the polarization spectra. The polarimetric data are indicative of a preferred axis in the stellar wind very close to the star, which is nearly perpendicular to the bipolar jet and almost parallel to the major axis of the elliptical ring nebula. This suggests a causal connection between the geometries seen on small and large scales in the circumstellar environment of AG Car.

We thank the staff of the Anglo-Australian Observatory, particularly J. Bailey, for their help with the observations and data

reduction. Data analysis was performed with a software package developed at the University of Wisconsin by K. H. Nordsieck and M. R. Meade. M. R. Meade, T. L. Smith, and A. Vaidya assisted with various aspects of the data analysis. This research made use of the Simbad database, operated at CDS, Strasbourg, France. We acknowledge many useful discussions with B. R. Espey. R. S.-L. and G. C. C. thank R. Cannon for granting a director's night at the AAT. This work was supported by NAS 2-56777, NAGW-2338, and NAGW-2977, and a travel grant from NOAO.

## REFERENCES

- Appenzeller, I. 1966, *Z. Astrophys.*, 64, 269  
 Barbier, R., & Swings, J. P. 1981, in *IAU Symp. 98, Be Stars*, ed. M. Jaschek & H. G. Groth (Dordrecht: Reidel), 103  
 Bernat, A. P., & Lambert, D. L. 1978, *PASP*, 90, 520  
 Bjorkman, J. E., & Cassinelli, J. P. 1993, *ApJ*, 409, 429  
 Brown, J. C., & McLean, I. S. 1977, *A&A*, 57, 141  
 Brown, J. C., McLean, I. S., & Emslie, A. G. 1978, *A&A*, 68, 415  
 Caputo, F., & Viotti, R. 1970, *A&A*, 7, 266  
 Cassinelli, J. P., Nordsieck, K. H., & Murison, M. A. 1987, *ApJ*, 317, 290  
 Clampin, M., Nota, A., Golimowski, D. A., Leitherer, C., & Durrance, S. T. 1993b, *ApJ*, 410, 35  
 Clayton, G. C., et al. 1992, *ApJ*, 385, 53  
 Conti, P. S. 1984, in *IAU Symp. 105, Observational Tests of Stellar Evolution Theory*, ed. A. Maeder & A. Renzini (Dordrecht: Reidel), 233  
 de Freitas Pacheco, J. A., Neto, A. D., Costa, R. D. D., & Viotti, R. 1992, *A&A*, 266, 360  
 Fox, G. K. 1991, *ApJ*, 379, 663  
 Hamann, F., De Poy, D. L., Johansson, S., & Elias, J. 1994, *ApJ*, 422, 626  
 Hillier, D. J. 1991, *A&A*, 247, 455  
 ———. 1992, in *Atmospheres of Early-Type Stars*, ed. U. Heber & C. S. Jeffrey (Berlin: Springer) 105  
 ———. 1994, *A&A*, in press  
 Hillier, D. J., & Allen, D. A. 1992, *A&A*, 262, 153  
 Hillier, D. J., McGregor, P. G., & Hyland, A. R. 1988, in *Mass Outflows from Stars and Galactic Nuclei*, ed. L. Bianchi & R. Gilmozzi (Dordrecht: Kluwer), 215  
 Höflich, P. 1991, *A&A*, 246, 481  
 Hoekzema, N., Lamers, H. J. L. M., & van Genderen, A. M. 1992, *A&A*, submitted  
 Hubeny, I., & Leitherer, C. 1989, *PASP*, 101, 114  
 Humphreys, R. M., & Davidson, K. 1979, *ApJ*, 232, 409  
 Humphreys, R. M., Lamers, H. J. L. M., Hoekzema, N., & Cassatella, A. 1989, *A&A*, 218, L17  
 Hutsemékers, D., & Kohoutek, L. 1988, *A&AS*, 73, 217  
 Kilmartin, P. M., & Bateson, F. M. 1991, *IAU Circ.* 5307  
 Lamers, H. J. G. L. M. 1987, in *Instabilities in Luminous Early Type Stars*, ed. H. J. G. L. M., Lamers, & C. W. H. de Loore (Dordrecht: Reidel), 99  
 Lamers, H. J. G. L. M., & de Loore, C. W. H. 1987, *Instabilities in Luminous Early Type Stars* (Dordrecht: Reidel)  
 Leitherer, C., et al. 1992a, *IAU Circ.* 5572  
 Leitherer, C., Neto, A. D., & Schmutz, W. 1992b, in *Nonisotropic and Variable Outflows from Stars*, ed. L. Drissen, C. Leitherer, & A. Nota (Provo: Brigham Young Univ. Press), 366  
 Leitherer, C., Schmutz, W., Abbott, D. C., Hammann, W.-R., & Wessolowski, U. 1989, *ApJ*, 346, 919  
 Maeder, A. 1990, *A&AS*, 84, 139  
 Maheswaran, M., & Cassinelli, J. 1994, *ApJ*, 421, 718  
 Mayall, M. 1969, *CJRAS*, 63, 221  
 McGregor, P. J., Finlayson, K., Hyland, A. R., Joy, M., Harvey, P. M., & Lester, D. F. 1988, *ApJ*, 329, 874  
 McLean, I. S., & Clarke, D. 1979, *MNRAS*, 186, 245  
 Mitra, M. P., & Dufour, R. J. 1990, *MNRAS*, 242, 98  
 Nota, A., Leitherer, C., Clampin, M., Greenfield, P., & Golimowski, D. A. 1992, *STScI preprint* 649  
 Paresce, F., & Nota, A. 1989, *ApJ*, 341, 83  
 Poe, C. H., Friend, D. B., & Cassinelli, J. P. 1989, *ApJ*, 337, 888  
 Poeckert, R., & Marlborough, J. M. 1978, *ApJ*, 220, 940  
 Robberto, M., Ferrari, A., Nota, A., & Paresce, F. 1993, *A&A*, 269, 330  
 Rudy, R. J. 1978, *PASP*, 90, 668  
 Schmid-Burgk J. 1982, *A&A*, 108, 169  
 Schulte-Ladbeck, R. E., Leitherer, C., Clayton, G. C., Robert, C., Meade, M. R., Drissen, L., Nota, A., & Schmutz, W. 1993, *ApJ*, 407, 723  
 Schulte-Ladbeck, R. E., Meade, M. R., & Hillier, D. J. 1992a, in *Nonisotropic and Variable Outflows from Stars*, ed. L. Drissen, C. Leitherer, & A. Nota (Provo: Brigham Young Univ. Press), 118  
 Schulte-Ladbeck, R. E., Nordsieck, K. H., Nook, M. A., Magalhães, A. M., Taylor, M., Bjorkman, K. S., & Anderson, C. M. 1990, *ApJ*, 365, 19  
 Schulte-Ladbeck, R. E., Nordsieck, K. H., Taylor, M., Bjorkman, K. S., Magalhães, A. M., & Wolff, M. J. 1992b, *ApJ*, 387, 347  
 Serkowski, K. 1968, *ApJ*, 154, 115  
 ———. 1970, *ApJ*, 160, 1083  
 Serkowski, K., Mathewson, D. S., & Ford, V. L. 1975, *ApJ*, 196, 261  
 Shields, G. A., & McKee, C. F. 1981, *ApJ*, 246, 57  
 Smith, L. J. 1991, in *IAU Symp. 143, Wolf-Rayet Stars and Interpretations with Other Massive Stars in Galaxies*, ed. K. A. van der Hucht & B. Hidayat (Dordrecht: Kluwer), 385  
 Smith, L. J., Crowther, P. A., & Prinja, R. K. 1994, *A&A*, in press  
 Sreenivasan, S. R., & Wilson, W. J. F. 1989, in *IAU Colloq. 113, Physics of Luminous Blue Variables*, ed. K. Davidson, A. F. J. Moffat, & H. J. G. L. M. Lamers (Dordrecht: Kluwer), 205  
 Stahl, O. 1987, *A&A*, 182, 229  
 Taylor, M., & Cassinelli, J. P. 1992, *ApJ*, 401, 311  
 Taylor, M., Nordsieck, K. H., Schulte-Ladbeck, R. E., & Bjorkman, K. S. 1991, *AJ*, 102, 1197  
 Thackeray, A. D. 1950, *MNRAS*, 110, 524  
 ———. 1977, *MNRAS*, 180, 95  
 Underhill, A. B., & Fahey, R. P. 1984, *ApJ*, 280, 712  
 Viotti, R., Altamore, A., Barklay, M., Cassatella, A., Gilmozzi, R., & Rossi, C. 1984, in *Future of Ultraviolet Astronomy Based on Six Years of IUE* (NASA CP-2349), 231  
 Viotti, R., Cassatella, A., Ponz, D., & Thé, P. S. 1988, *A&A*, 190, 333  
 Warren-Smith, R. F., Scarrott, S. M., Murdin, P., & Bingham, R. G. 1979, *MNRAS*, 187, 761  
 Whittet, D. C. B., Martin, P. G., Hough, J. H., Rouse, M. F., Bailey, J. A., & Axon, D. J. 1992, *ApJ*, 386, 562  
 Wilking, B. A., Lebofsky, M. J., & Rieke, G. H. 1982, *AJ*, 87, 695  
 Wolf, B., & Stahl, O. 1982, *A&A*, 112, 111  
 Wood, K., Brown, J. C., & Fox, G. K. 1993, *A&A*, 271, 492